Accepted Manuscript

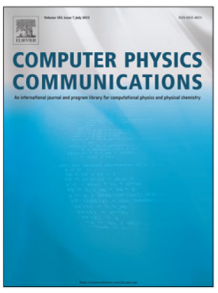

Local structure-preserving algorithms for general multi-symplectic Hamiltonian PDEs

Jiaxiang Cai, Yushun Wang, Chaolong Jiang

PII: S0010-4655(18)30311-4
DOI: https://doi.org/10.1016/j.cpc.2018.08.015
Reference: COMPHY 6598

To appear in: *Computer Physics Communications*

Received date : 28 November 2017
Revised date : 13 August 2018
Accepted date : 31 August 2018

Please cite this article as: J. Cai, Y. Wang, C. Jiang, Local structure-preserving algorithms for general multi-symplectic Hamiltonian PDEs, *Computer Physics Communications* (2018), https://doi.org/10.1016/j.cpc.2018.08.015

Local structure-preserving algorithms for general multi-symplectic Hamiltonian PDEs

Jiaxiang Cai[a,*], Yushun Wang[b], Chaolong Jiang[b]

[a]School of Mathematical Science, Huaiyin Normal University, Huaian, Jiangsu 223300, China.

[b]Jiangsu Key Laboratory for NSLSCS, School of Mathematical Sciences, Nanjing Normal University, Nanjing 210046, China.

Abstract

Many PDEs can be recast into the general multi-symplectic formulation possessing three local conservation laws. We devote the present paper to some systematic methods, which hold the discrete versions of the local conservation laws respectively, for the general multi-symplectic PDEs. For the original problem subjected to appropriate boundary conditions, the proposed methods are globally conservative. The proposed methods are successfully applied to many one-dimensional and multi-dimensional Hamiltonian PDEs, such as KdV equation, G-P equation, Maxwell's equations and so on. Numerical experiments are carried out to verify the theoretical analysis.

keywords: Multi-symplectic Hamiltonian PDE, structure-preserving algorithm, conservation law, discrete gradient, dispersion relation

1 Introduction

A wide range of d-dimensional PDEs can be written into a multi-symplectic Hamiltonian form [1]

$$M\partial_t z + \sum_{l=1}^{d} K_l \partial_{x_l} z = \nabla_z S(z), \quad z \in \mathbb{R}^{d_1}, \tag{1}$$

where M and K_l, $l = 1, 2, \ldots, d$, are constant $d_1 \times d_1$ skew-symmetric matrices, $z = z(t, \mathbf{x})$, $\mathbf{x} = (x_1, x_2, \ldots, x_d)$, is a state variable, and $S : \mathbb{R}^{d_1} \to \mathbb{R}$ is a scalar-valued smooth function, such as the Sine-Gordon equation [2], the Korteweg-de Vries (KdV) equation [3], the Camassa-Holm equation [4], the regularized long-wave (RLW) equation [5], the nonlinear Schrödinger (NLS) equation [6,7], Maxwell's equations [8,9] and so on. It is well-known that the solution z of (1) admits a multi-symplectic conservation law (MSCL)

$$\partial_t \omega + \sum_{l=1}^{d} \partial_{x_l} \kappa_l = 0, \tag{2}$$

with the differential 2-form $\omega = dz \wedge \widehat{M} dz$ and $\kappa_l = dz \wedge \widehat{K}_l dz$ where matrices $\widehat{M}$ and $\widehat{K}_l$ satisfy

$$M = \widehat{M} - \widehat{M}^T, \quad K_l = \widehat{K}_l - \widehat{K}_l^T. \tag{3}$$

A numerical method that satisfies a discrete version of (2) is called multi-symplectic integrator; see [2] for reviews of multi-symplectic integration. Up to now, some multi-symplectic integrators have been proposed for the multi-symplectic Hamiltonian PDEs and exhibit good numerical performances, such as the box scheme obtained by applying simply implicit midpoint rule (a Runge-Kutta method) in both time and space [2], the Euler-box scheme developed by using the non-compact Euler rule in both time and space [10], the pseudospectral scheme obtained by applying the pseudospectral method in space and the implicit midpoint rule in time [11], and the diamond scheme [12]. Although multi-symplecticity by itself does not ensure good performance on traditional criteria like accuracy and stability, multi-symplectic methods do have a number of advantages. On the one hand, they are essentially variational and the

*Corresponding author. E-mail address: cjx1981@hytc.edu.cn, thomasjeer@sohu.com.

standard discrete model in the relevant part of physics. On the other hand, the symplecticity in space is essential for a semidiscretization to be amenable to symplectic time integration, whose advantages in long-time integration are well known, and the symplecticity in space can also preserve periodic, quasi-periodic and heteroclinic solutions. However, multi-symplectic integrators can only preserve some conservation laws, and these do not typically include those of energy and momentum, which can be important for nonlinear stability and the nonlinear convergence analysis of the schemes.

In recent years, there has been an increased emphasis on constructing numerical methods preserving certain invariant quantities such as energy and momentum in the continuous dynamical systems. Nowadays, for computing physical/chemical problem, whether the numerical scheme captures the energy/momentum of the system has been a criterion to judge the success of the numerical simulation. Many PDEs with appropriate boundary conditions admit the global energy/momentum conservation law and there have been some techniques for constructing the global energy-/momentum-preserving methods for these conservative PDEs [13–15]. However, these discrete preserving properties are global and depend on the boundary conditions inevitably, so that the schemes are invalid for the problem without appropriate boundary conditions. As we known, besides possessing the global conservation laws, many PDEs also have local conservation laws which are independent of the boundary conditions and more essential than the global ones. For example, the multi-symplectic Hamiltonian PDE admits a local energy conservation law (LECL)

$$\partial_t E + \sum_{l=1}^{d} \partial_{x_l} F_l = 0, \tag{4}$$

where $E = S(z) + \sum_{l=1}^{d} (\partial_{x_l} z)^T \widehat{K}_l z$ and $F_l = -(\partial_t z)^T \widehat{K}_l z$ represent the energy density and energy fluxes respectively, and also has local momentum conservation laws (LMCLs) in the x_l directions , $l = 1, 2, \ldots, d$, given by

$$\partial_t I_l + \partial_{x_l} G_l + \sum_{j=1, j\neq l}^{d} \partial_{x_j} \tilde{G}_{l,j} = 0, \tag{5}$$

where $I_l = -(\partial_{x_l} z)^T \widehat{M} z$, $G_l = S(z) + (\partial_t z)^T \widehat{M} z + \sum_{j=1, j\neq l}^{d} (\partial_{x_j} z)^T \widehat{K}_j z$ and $\tilde{G}_{l,j} = -(\partial_{x_l} z)^T \widehat{K}_j z$. It is clear that the local conservation laws (4) and (5) are established on any time-space point and independent of boundary conditions. Assume that the PDEs are imposed on some appropriate boundary conditions, these LECL and LMCLs will result in global energy and momentum conservation laws, respectively. And thus the LECL and LMCLs produce richer informations of the PDE system than the corresponding global ones. Naturally, we expect to propose a scheme that satisfies a discrete version of LECL (4) or LMCL (5). In this paper, this kind of schemes will be called local energy-preserving (LEP) integrator or local momentum-preserving (LMP) integrator. On the construction of the LEM and LMP integrators for the PDEs, we have done some works. In [16,17], by using the concatenating method, we have proposed some LEP and LMP schemes for the Sine-Gordon equation and the coupled NLS equations. These schemes have excellent properties and exhibit good numerical performance, but they are not completely systematic either in their derivations or in their applicability to a class of PDEs. Recently, combining the implicit midpoint rule with the averaged vector field (AVF) method, we have developed a LEP integrator and a LMP integrator which are applicable to the entire class (1) in one dimension [18]. The derivation of the LEP and LMP schemes are easy, however, these schemes have some less positive features. The schemes are fully implicit, which makes them expensive; The implicit equations may not have a solution: with periodic boundary conditions, solvability requires that the number of grid points be odd [19]; For a given PDE, it is difficult to establish the error estimates of the obtained LEP/LMP scheme no matter whether there exist positive invariants or not. The reason is that there is no relationship $c_1\|e^n\| \leq \|A_x e^n\| \leq c_2\|e^n\|$, where constants c_1, $c_2 > 0$, $\|\cdot\|$ represents the discrete l_2-norm, A_x is an average operator, and e^n represents the error vector whose entries denote the difference between the numerical solution of the LEP/LMP scheme and the exact solution of original problem.

In this paper, instead of discretizing one particular PDE, we wish to develop methods that are applicable to the entire class of multi-symplectic Hamiltonian PDEs (1), specializing to a particular equation or family as late as possible. To this end, we split the skew-symmetric matrix M or K_l in the form of (3). And then applying the leap-frog rule to space/time gives a semi-discrete system of ODEs with respect to time/space. Next, we use a discrete gradient (DG) method such as the coordinate increment DG method [20], the midpoint DG method [21], or the AVF method to integrate the obtained ODEs.

In this study, an application of the AVF method gives a fully discrete LEP/LMP scheme for the multi-symplectic Hamiltonian PDE (1). The AVF method was first written down in [22] for the system of ODEs $dy/dt = f(y)$, $y \in \mathbb{R}^d$, and identified as an energy-preserving and B-series method in [23]. The second-order AVF method is the map $y_n \longmapsto y_{n+1}$ defined by

$$\frac{y_{n+1} - y_n}{\tau} = \int_0^1 f((1-\xi)y_n + \xi y_{n+1})\mathrm{d}\xi, \tag{6}$$

where τ is the step size. The method (6) is affine-covariant [24] and self-adjoint. When f is Hamiltonian with respect to a constant symplectic structure, i.e., $f = S^{-1}\nabla H$ with S a nonsingular and antisymmetric matrix, the AVF method preserves the Hamiltonian $H : \mathbb{R}^{d_1} \to \mathbb{R}$. Besides preserving the LECL or LMCL of the system (1), the present method also has several appealing properties. It is systematic and applicable to a huge of PDEs which has the multi-symplectic Hamiltonian form (1); Applications of the matrix splitting technique and leap-frog rule may result in an fully explicit or linearly implicit scheme for some nonlinear PDEs; Different schemes can be proposed due to different splitting matrices; The method is effective and valid no matter whether the number of the grid points is odd or even; The present method is established on the grid points unlike the method in [18] establishing on the central box, so that the discrete conservation laws are also related to the grid points. For some particular multi-symplectic Hamiltonian PDEs holding the positive discrete conservation laws, the feature allows us to establish the error estimate of the scheme easily.

The present work is organized as follows. In section 2, we briefly review the multi-symplectic form of the one-dimensional PDE and then develop a class of energy- and momentum-preserving integrators for it. We apply the developed local structure-preserving integrators to some classical one-dimensional PDEs and conduct numerical experiments to show their numerical performance in the same section. In section 3, the methodology of the local structure-preserving algorithms for the one-dimensional multi-symplectic Hamiltonian PDE is extended to multi-dimensional multi-symplectic Hamiltonian PDEs. In section 4, we study the LEP discretization by means of numerical dispersion relation for the linear PDE. Finally, we finish the paper with concluding remarks in section 5.

2 Local structure-preserving algorithms for 1D problem

Consider the multi-symplectic Hamiltonian PDE (1) in one dimension ($d = 1$), i.e.,

$$M\partial_t z + K\partial_x z = \nabla_z S(z), \quad z \in \mathbb{R}^{d_1}, \tag{7}$$

where $(x,t) \in [a,b] \times [0,T]$. When dealing with (semi-)discrete systems we use the notation u_j^n where the index j corresponds to increments in space and n to increments in time. That is, the point u_j^n is the discrete equivalent of $u(a+jh, n\tau)$, where $h = (b-a)/J$ and $\tau = T/N$. Define the finite difference operators $\delta_t^{\pm} f_j^n = \pm(f_j^{n\pm1} - f_j^n)/\tau$, $\delta_x^{\pm} f_j^n = \pm(f_{j\pm1}^n - f_j^n)/h$, and the average operators $A_t f_j^n = (f_j^{n+1} + f_j^n)/2$, $A_x f_j^n = (f_{j+1}^n + f_j^n)/2$. It is easy to check that the operators are commutative and admit discrete Leibnitz rules

$$\delta_x^+(f_{j-1}^n g_j^n) = f_j^n \cdot \delta_x^+ g_j^n + \delta_x^- f_j^n \cdot g_j^n$$

and $\delta_x^+(f \cdot g)_j^n = \delta_x^+ f_j^n \cdot A_x g_j^n + A_x f_j^n \cdot \delta_x^+ g_j^n$. One can obtain analogous versions in the time direction.

2.1 Local energy-preserving method

Let $\widehat{K}$ be a splitting matrix of M, satisfying the relation (3). For the 1D multi-symplectic Hamiltonian PDE (7), we make a spatial discretization as follows:

$$M\frac{d}{dt}z_j + \widehat{K}\delta_x^+ z_j - \widehat{K}^T\delta_x^- z_j = \nabla_z S(z_j), \quad j = 0, 1, \cdots, J-1. \tag{8}$$

Taking the inner product of (8) with dz_j/dt on both sides together with the vanishment of $(dz_j/dt)^T M(dz_j/dt)$, we have

$$(\frac{d}{dt}z_j)^T\widehat{K}\delta_x^+ z_j - (\frac{d}{dt}z_j)^T\widehat{K}^T\delta_x^- z_j = \frac{d}{dt}S(z_j). \tag{9}$$

The left-hand terms can be reformed into $\delta_x^+(dz_{j-1}/dt)^T\widehat{K}z_j - d((\delta_x^- z_j)^T\widehat{K}z_j)/dt$. And thus it follows from (9) that

$$dE_j/dt + \delta_x^+ F_j = 0, \quad E_j = S(z_j) + (\delta_x^- z_j)^T\widehat{K}z_j, \quad F_j = -(dz_{j-1}/dt)^T\widehat{K}z_j. \tag{10}$$

This is a local property, independent of boundary conditions, which shows that the semi-discrete system (8) conserves the semi-discrete energy conservation law exactly. Next, an application of a DG method to (8) gives a fully discrete scheme

$$M\delta_t^+ z_j^n + \widehat{K}A_t\delta_x^+ z_j^n - \widehat{K}^T A_t\delta_x^- z_j^n = \overline{\nabla}_z S\left(z_j^{n+1}, z_j^n\right), \tag{11}$$

where $\overline{\nabla}_z$ is a DG of S, that is, a continuous function of $(\hat{z}, z)$ satisfying $\overline{\nabla}_z S(\hat{z}, z)^T(\hat{z} - z) = S(\hat{z}) - S(z)$ and $\overline{\nabla}_z S(z, z) = \nabla_z S(z)$.

Theorem 2.1. *The method (11) possesses a discrete local energy conservation law*

$$\delta_t^+ E_j^n + \delta_x^+ F_j^{n+\frac{1}{2}} = 0, \tag{12}$$

where $E_j^n = S(z_j^n) + (\delta_x^- z_j^n)^T\widehat{K}z_j^n$ *and* $F_j^{n+\frac{1}{2}} = -(\delta_t^+ z_{j-1}^n)^T\widehat{K}(A_t z_j^n)$.

Proof. Left-multiplying (14) with $(\delta_t^+ z_j^n)^T$ on both sides reads

$$(\delta_t^+ z_j^n)^T(\widehat{K}A_t\delta_x^+ z_j^n - \widehat{K}^T A_t\delta_x^- z_j^n) = (\delta_t^+ z_j^n)^T\overline{\nabla}_z S\left(z_j^{n+1}, z_j^n\right). \tag{13}$$

The right-hand term can be written into $\delta_t^+ S(z_j^n)$, and by the discrete Leibnitz rules, the left-hand term becomes

$$\begin{aligned}&(\delta_t^+ z_j^n)^T\widehat{K}A_t\delta_x^+ z_j^n - \delta_t^+((\delta_x^- z_j^n)^T\widehat{K}z_j^n) + (\delta_t^+\delta_x^- z_j^n)^T\widehat{K}A_t z_j^n\\ =&\delta_x^+((\delta_t^+ z_{j-1}^n)^T\widehat{K}A_t z_j^n) - \delta_t^+((\delta_x^- z_j^n)^T\widehat{K}z_j^n).\end{aligned}$$

This completes the proof. □

In particular, integrating (8) by the second-order AVF method gives a discrete scheme

$$M\delta_t^+ z_j^n + \widehat{K}A_t\delta_x^+ z_j^n - \widehat{K}^T A_t\delta_x^- z_j^n = \int_0^1 \nabla_z S\left((1-\xi)z_j^n + \xi z_j^{n+1}\right)\mathrm{d}\xi. \tag{14}$$

Remark 1. 1. In this paper, the second-order AVF method is employed to integrate the system (8). Other DG methods such as the coordinate increment DG method, midpoint DG method and fourth-order AVF method can also be employed. 2. The discrete LECL is consistent with the continuous version (4) in one dimension. The exact preservation of the discrete version of (4) indicates that the proposed method can produce richer information of the original system. 3. For some particular multi-symplectic Hamiltonian PDEs, different splitting matrix $\widehat{K}$ may lead to different LEP schemes.

Corollary 2.1. *If the multi-symplectic Hamiltonian PDE (7) is subjected to appropriate boundary conditions, such as periodic/homogeneous boundary conditions, the proposed LEP scheme will preserve a discrete global energy conservation law* $\mathcal{E}^n = h\sum_j E_j^n = \mathcal{E}^{n-1} = \cdots = \mathcal{E}^0$.

2.2 Local momentum-preserving method

In the previous section, we propose a systematic LEP integrator that is applicable to the entire class of multi-symplectic Hamiltonian PDE (7). As we known, the system (7) also admits LMCLs (see (5) with $d = 1$). Momentum conservation laws also play an important role in the physical research, however the works on construction of the momentum-preserving scheme for the multi-symplectic Hamiltonian system are a few. Although the multi-symplectic box scheme is momentum-preserving as the boundary conditions are periodic, it is not local momentum-preserving. Next, the idea of construction of the LEP integrator will be extended to develop the LMP integrator for the system (7).

Let $\widehat{M}$ be a splitting matrix of M, satisfying (3), and then make a temporal semi-discretiztion

$$\widehat{M}\delta_t^+ z^n - \widehat{M}^T\delta_t^- z^n + K\frac{d}{dx}z^n = \nabla_z S(z^n), \tag{15}$$

for the system (7). It is easy to show that the semi-discrete scheme (15) has a LECL

$$\delta_t^+ I^n + \frac{d}{dx}G^n = 0, I^n = -(\frac{d}{dx}z^{n-1})^T\widehat{M}z^n, G^n = S(z^n) + (\delta_t^- z^n)^T\widehat{M}z^n, \tag{16}$$

which is independent of boundary conditions. For the semi-discrete system (15), an application of the AVF method in space yields

$$\widehat{M}\delta_t^+ A_x z_j^n - \widehat{M}^T\delta_t^- A_x z_j^n + K\delta_x^+ z_j^n = \int_0^1 \nabla_z S((1-\xi)z_j^n + \xi z_{j+1}^n)\mathrm{d}\xi. \tag{17}$$

It is worthy to note that the nonlinear term only contains the values of numerical solution at n-th time level. And thus it is an explicit scheme. As in the proof of Theorem 2.1, it is easy to prove the scheme (17) has the following discrete LMCL.

Theorem 2.2. *The method (17) is local momentum-preserving, which satisfies a discrete LECL*

$$\delta_t^+ I_{j+1/2}^n + \delta_x^+ G_j^n = 0, \tag{18}$$

where $I_{j+1/2}^n = -(\delta_x^+ z_j^{n-1})^T\widehat{M}A_x z_j^n$ *and* $G_j^n = S(z_j^n) + (\delta_t^- z_j^n)^T\widehat{M}z_j^n$.

Corollary 2.2. *If the multi-symplectic Hamiltonian PDE (7) is subjected to the periodic/homogeneous boundary conditions, the LMP integrator (17) conserves a discrete global momentum conservation law* $\mathcal{I}^n = h\sum_j I_{j+1/2}^n = \mathcal{I}^{n-1} = \cdots = \mathcal{I}^0$.

2.3 Applications

Many 1D PDEs motivated by physics can be stated as (7). Here, we consider the KdV equation, RLW equation, Sine-Gordon equation and NLS equation, which are important models in physics and engineering. Next, we first write the given 1D PDEs into the multi-symplectic Hamiltonian form of (7), and then respectively apply the LEP (14) and LMP (17) integrators to them. To show the robustness and effectiveness of the proposed integrators, we solve these equations imposed on different boundary conditions.

Example 1. The KdV equation, given by

$$u_t + \eta u u_x + \mu^2 u_{xxx} = 0,$$

is of the form (7) with $S(z) = v^2/2 - uw + \eta u^3/6$, $z = (\phi, u, v, w)^T$ and

$$M = \begin{pmatrix} 0 & 1/2 & 0 & 0 \\ -1/2 & 0 & 0 & 0 \\ 0 & 0 & 0 & 0 \\ 0 & 0 & 0 & 0 \end{pmatrix},\ K = \begin{pmatrix} 0 & 0 & 0 & 1 \\ 0 & 0 & -\mu & 0 \\ 0 & \mu & 0 & 0 \\ -1 & 0 & 0 & 0 \end{pmatrix}.$$

Take $\widehat{K}$ as a lower triangular matrix of the matrix K. An application of the LEP integrator (14) to the multi-symplectic form gives

$$\begin{cases} \frac{1}{2}\delta_t^+ u_j^n + A_t\delta_x^- w_j^n = 0, \\ -\frac{1}{2}\delta_t^+ \phi_j^n - \mu A_t\delta_x^- v_j^n = -A_t w_j^n + \eta f(u_j^{n+1}, u_j^n), \\ \mu A_t\delta_x^+ u_j^n = A_t v_j^n, \\ A_t\delta_x^+ \phi_j^n = A_t u_j^n, \end{cases} \tag{19}$$

where $f(r,s) = (r^2 + rs + s^2)/6$. Because $\mu u_x = v$ and $\phi_x = u$ contain no time derivative, so it can be more accurately discretized by omitting the time average operator A_t in the last two equations of (19) to

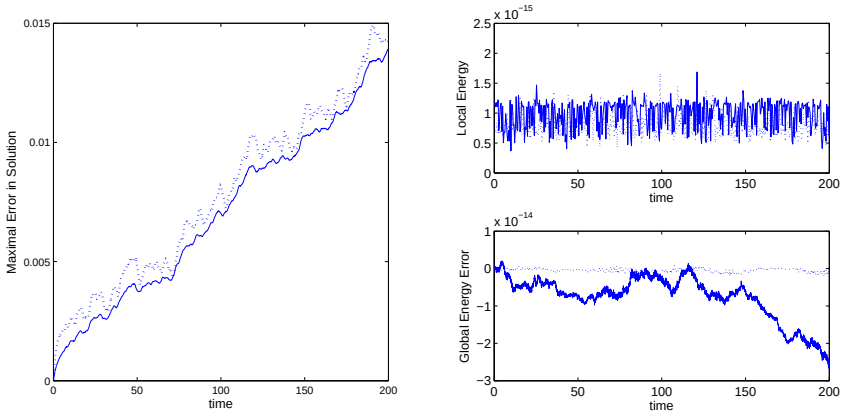

Figure 1: The numerical results for the KdV equation ($\eta = \mu = 1$) obtained by the schemes (20) (solid line) and (21) (dotted line). Left: the maximal error in solution. Right-top: local energy. Right-bottom: global energy error.

Table 1: Numerical results for the KdV equation: $\tau = 0.05$, $h = 40/201$ and $T = 100$.

Results\Scheme	LEP (20)	LEP (21)	LEP [18]	MPS [25]	NBS [26]
L_∞-error	7.01e-3	8.14e-3	6.44e-3	6.45e-3	7.01e-3
$\lvert\mathcal{E}^n - \mathcal{E}^0\rvert$	8.66e-15	3.33e-16	1.97e-13	1.77e-6	3.27e-4
CPU time	2.25s	2.37s	3.32s	2.61s	2.33s

give $\mu\delta_x^+ u_j^n = v_j^n$ and $\delta_x^+ \phi_j^n = u_j^n$. Eliminating the auxiliary variables w_j^n, v_j^n and w_j^n yields a two-time level LEP scheme

$$\frac{1}{2}\delta_t^+ u_{j-1}^n + \frac{1}{2}\delta_t^+ u_j^n + \mu^2 \delta_x^+ \delta_x^- \delta_x^- A_t u_j^n + \eta \delta_x^- f(u_j^{n+1}, u_j^n) = 0. \tag{20}$$

Generally, different splitting matrices may read different schemes. Choosing $\widehat{K}$ as an upper triangular matrix of the matrix K yields a same scheme as (20), while $\widehat{K} = K/2$ gives a different LEP scheme

$$\delta_t^+ u_j^n + \mu^2 \bar{\delta}_x^3 A_t u_j^n + \eta \bar{\delta}_x f(u_j^{n+1}, u_j^n) = 0, \tag{21}$$

where $\bar{\delta}_x = (\delta_x^+ + \delta_x^-)/2$.

The KdV equation admits an analytic solution $u(x,t) = 3c\mathrm{sech}^2(\frac{\sqrt{c}}{2}(x - ct - x_0))$, $c > 0$, which represents the soliton moves to right with velocity c and amplitude $3c$. Consider the initial data $u_0(x) = u(x,0)$ with $-20 \le x \le 20$, $c = 1/3$, $x_0 = 0$ and periodic boundary conditions. The simulations are carried out on the equispaced spatial mesh ($h = 0.2$) up to $T = 200$ with $\tau = 0.05$ (the outgoing soliton comes back to the interval from the left boundary because of the periodic boundary conditions). Fig. 1 shows the numerical results obtained by the LEP schemes (20) and (21). From the left graph, one can see that the growth of maximal errors in solution is oscillatory and the solution errors seem to be quite close. The two schemes provide accurate solutions in long-term simulation (the solution errors are smaller than 0.015 at $T = 200$). From the right graphs, one can see that both the local energy and the error in global energy oscillate and stay around zero. These results strongly suggest that the two schemes capture both the local and global energies exactly. The results coincide with the theoretical ones.

Next, we make some numerical comparisons with the second-order finite difference schemes, including the LEP scheme [18], multisymplectic Preissmann scheme (MPS) [25] and narrow box scheme (NBS) [26]. The results in Table 1 show that all the schemes have comparative solution accuracies and computational efficiency, while the LEP schemes have exact preservation of the global energy.

Remark 2. At n-th time level, the value of local energy is scaled by $\max_j |\delta_t^+ E_j^n + \delta_x^+ F_j^{n+1/2}|$, and the error in global energy is monitored by $\mathcal{E}^n - \mathcal{E}^0$.

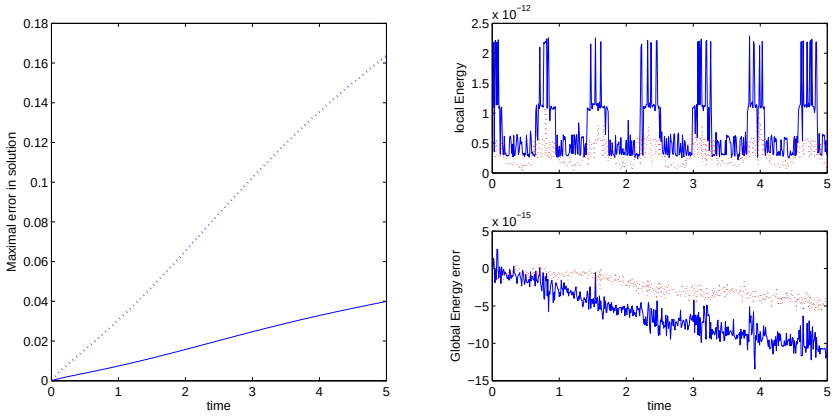

Figure 2: The numerical results for NLS equation obtained by schemes (23) (solid line) and (24) (dotted line). Left: maximal error in solution ψ. Right-top: local energy. Right-bottom: global energy error.

Example 2. The time-dependent NLS equation is $i\psi_t + \psi_{xx} + a|\psi|^2\psi = 0$. We set $\psi(x,t) = p(x,t) + iq(x,t)$ and then write the NLS equation into the multi-symplectic Hamiltonian form (7) with $S(z) = \frac{1}{2}(v^2 + w^2 + \frac{a}{2}(p^2+q^2)^2)$, $z = (p,q,v,w)^T$ and

$$M = \begin{pmatrix} J & 0 \\ 0 & 0 \end{pmatrix}, K = \begin{pmatrix} 0 & -I \\ I & 0 \end{pmatrix}, J = \begin{pmatrix} 0 & 1 \\ -1 & 0 \end{pmatrix}, I = \begin{pmatrix} 1 & 0 \\ 0 & 1 \end{pmatrix}.$$

The choice of $\widehat{K}$ as a lower triangular matrix of K yields

$$\begin{cases} \delta_t^+ q_j^n - A_t \delta_x^- v_j^n = a g_1(p_j^{n+1}, p_j^n, q_j^{n+1}, q_j^n), \\ -\delta_t^+ p_j^n - A_t \delta_x^- w_j^n = a g_1(q_j^{n+1}, q_j^n, p_j^{n+1}, p_j^n), \\ A_t \delta_x^+ p_j^n = A_t v_j^n, \\ A_t \delta_x^+ q_j^n = A_t w_j^n, \end{cases} \tag{22}$$

where $g_1(r_1, r_2, s_1, s_2) = \frac{1}{4}(r_1+r_2)(r_1^2+r_2^2+s_1^2+s_2^2) + \frac{1}{6}(s_1-s_2)(r_1 s_2 - r_2 s_1)$. Omitting the operator A_t in the third and fourth lines of (22), and then eliminating the auxiliary variables give the following LEP scheme

$$i\delta_t^+ \psi_j^n + \delta_x^+ \delta_x^- A_t \psi_j^n + a g(\psi_j^{n+1}, \psi_j^n, p_j^{n+1}, p_j^n) = 0, \tag{23}$$

where $g(r_1, r_2, s_1, s_2) = \frac{1}{4}(r_1+r_2)(|r_1|^2 + |r_2|^2) + \frac{1}{6}(r_1 - r_2)(r_1 s_2 - r_2 s_1)$. In addition, a different choice of the splitting matrix $\widehat{K} = K/2$ results in another LEP scheme

$$i\delta_t^+ \psi_j^n + \bar{\delta}_x^2 A_t \psi_j^n + a g(\psi_j^{n+1}, \psi_j^n, p_j^{n+1}, p_j^n) = 0, \tag{24}$$

for the NLS equation

Consider the NLS problem ($a = 2$) with initial condition $\psi(x,0) = \mathrm{sech}(x)\exp(ix)$, $x \in [-20, 60]$ and periodic boundary condition. The equation admits an analytical solution $\psi(x,t) = \mathrm{sech}(x-2t)\exp(ix)$. Fig. 2 shows the numerical results by the two proposed schemes, where the time and space mesh widths are set to $\tau = 0.01$ and $h = 0.1$ respectively. From the figure, it is clear that the maximal errors in solution increase almost linearly (see left graph), and both the local and global energies are preserved exactly since their errors are always in the scale of the round-off error of the machine throughout computations (see the right graphs). Table 2 displays the numerical results of different local structure structure-preserving schemes. One can see that the LEP scheme (23) exhibits the best numerical performance. In addition, the LEP scheme (24) with central finite operator provides less accurate solution than the other schemes, which can also be confirmed by the L_∞-error result in Table 1.

Example 3. For the RLW equation $u_t + au_x - \delta u_{xxt} + \frac{\gamma}{2}(u^2)_x = 0$, by defining the potential $\varphi_x = u$, momentum $v = u_x$, and variables $\omega = u_t$ and $p = \varphi_t/2 + a\varphi_x/2 + \gamma\varphi_x^2/2 - \delta\varphi_{xxt}$, one obtains a

Table 2: Numerical results for the Schrödinger equation: $\tau = 0.01$, $h = 80/801$ and $T = 5$.

Results\Scheme	LEP (23)	LEP (24)	LEP [18]	LMP [18]
L_∞-error	3.98e-2	1.63e-1	1.12e-1	1.01e-1
$\lvert\mathcal{E}^n - \mathcal{E}^0\rvert$	2.49e-14	1.22e-14	6.99e-14	1.37e-3
CPU time	1.11s	1.20s	1.60s	1.84s

multi-symplectic Hamiltonian form [5] with $S(z) = up - \gamma u^3/6 + \delta v\omega/2$, $z = (\varphi, u, v, \omega, p)^T$ and

$$M = \begin{pmatrix} 0 & -\frac{a}{2} & 0 & 0 & 0 \\ \frac{a}{2} & 0 & -\frac{\delta}{2} & 0 & 0 \\ 0 & \frac{\delta}{2} & 0 & 0 & 0 \\ 0 & 0 & 0 & 0 & 0 \\ 0 & 0 & 0 & 0 & 0 \end{pmatrix}, \; K = \begin{pmatrix} 0 & -\frac{1}{2} & 0 & 0 & -1 \\ \frac{1}{2} & 0 & 0 & -\frac{\delta}{2} & 0 \\ 0 & 0 & 0 & 0 & 0 \\ 0 & \frac{\delta}{2} & 0 & 0 & 0 \\ 1 & 0 & 0 & 0 & 0 \end{pmatrix}.$$

Taking the splitting matrix $\widehat{K}$ as an upper/lower triangular matrix of K reads the two-time level LEP scheme

$$\delta_t^+ A_x u_{j-1}^n + aA_t\delta_x^- u_j^n - \frac{\delta}{2}\delta_t^+\delta_x^{-2} u_j^n - \frac{\delta}{2}\delta_t^+\delta_x^+\delta_x^- u_j^n + \gamma\delta_x^- f(u_j^{n+1}, u_j^n) = 0, \tag{25}$$

which is same as the LEP-II scheme in [27]. In Examples 2 and 3, the choice of $\widehat{K} = K/2$ or $\widehat{K}$ as an upper/lower triangular matrix of K has yielded different LEP schemes. In this example, we will consider another splitting matrix $\widehat{K}$ of K, given by

$$K = \begin{pmatrix} 0 & 0 & 0 & 0 & -1 \\ \frac{a}{2} & 0 & 0 & 0 & 0 \\ 0 & 0 & 0 & 0 & 0 \\ 0 & \frac{\delta}{2} & 0 & 0 & 0 \\ 0 & 0 & 0 & 0 & 0 \end{pmatrix}.$$

This choice results in a LEP scheme

$$\delta_t^+ A_x u_j^n + \frac{a}{2} A_t\delta_x^+ u_{j+1}^n + \frac{a}{2} A_t\delta_x^- u_j^n - \frac{\delta}{2}\delta_t^+\delta_x^{+2} u_j^n - \frac{\delta}{2}\delta_t^+\delta_x^+\delta_x^- u_j^n + \gamma\delta_x^+ f(u_j^{n+1}, u_j^n) = 0, \tag{26}$$

for the RLW equation, which is different to (25).

Next, we consider the LMP scheme for the RLW equation. Let $\widehat{M}$ be an upper triangular matrix of the matrix M. It follows from the LMP integrator (17) that

$$\begin{cases} \frac{1}{2}\delta_t^+ A_x u_j^n + \frac{a}{2}\delta_x^+ u_j^n + \delta_x^+ p_j^n = 0, \\ -\frac{1}{2}\delta_t^- A_x\varphi_j^n - \frac{\delta}{2}\delta_t^+ A_x v_j^n + \frac{a}{2}\delta_x^+\varphi_j^n - \frac{\delta}{2}\delta_x^+ w_j^n = A_x p_j^n - \gamma f(u_{j+1}^n, u_j^n), \\ \delta_t^- u_j^n = w_j^n, \\ \delta_x^+ u_j^n = A_x v_j^n, \\ \delta_x^+\varphi_j^n = A_x u_j^n, \end{cases} \tag{27}$$

which can be wirtten in an equivalent form

$$\bar{\delta}_t A_x^2 u_j^n + a\delta_x^+ A_x u_j^n - \delta\bar{\delta}_t\delta_x^{+2} u_j^n + \gamma\delta_x^+ f(u_{j+1}^n, u_j^n) = 0. \tag{28}$$

The following experiments are done to check the effectiveness of the proposed LEP and LMP schemes. The equation admits a theoretical solution $u(x,t) = 3c\mathrm{sech}^2(m(x - \nu t))$ with $\nu = \gamma c + a$ and $m = \sqrt{\gamma c/(\nu\delta)}/2$. In what follows, we consider the parameters $a = 1$, $\delta = 1$ and $\gamma = 1$, initial condition $u_0(x) = u(x, 0)$, $x \in [-60, 200]$ with $c = 1$ and homogeneous boundary condition $u(-60, t) = u(200, t) = 0$. The simulations are carried out with $\tau = 0.05$ and $h = 0.1$ up to $T = 100$. The numerical results are displayed in Fig. 3. From the left graph, it is clear that all schemes provide accurate solutions in long-term computation, and the solution errors of the LEP schemes are very close but smaller than that of LMP. The LEP and LMP schemes are global energy- and momentum-preserving respectively under the homogeneous boundary condition, which are verified by the results in middle and right graphs.

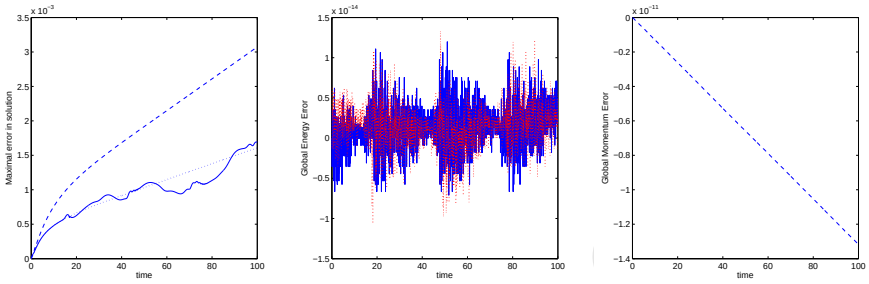

Figure 3: The numerical results for the RLW equation obtained by the LEP scheme (25) (solid line), the LEP scheme (26) (dotted line) and the LMP scheme (28) (dashed line). Left: the maximal error in solution. Middle: the global energy error of the LEP schemes. Right: the global momentum error.

Table 3: Numerical results of various schemes for the RLW equation.

Method	$\mathcal{I}_1$	$\mathcal{I}_3$	$L_2 \times 10^4$	$L_\infty \times 10^4$
LEP (25)	3.97995	0.42983	0.24	0.09
LEP (26)	3.97995	0.42983	0.24	0.09
LMP (28)	3.97997	0.42983	5.88	2.28
LEP [18]	3.97995	0.42983	0.78	0.31
LMP [18]	3.97997	0.42983	0.78	0.31
LEP-I [27]	3.97995	0.42983	0.78	0.31
LEP-III [27]	3.97995	0.42983	1.26	0.43
[5]	3.97993	0.42983	0.52	0.20
[28]	3.97988	0.42983	2.19	0.86
[29]	3.98203	0.42884	46.9	17.6
[30]	3.98206	0.43022	5.11	1.98
[31]	3.97804	0.42943	5.32	2.27
[32]	3.97781	0.42937	5.15	1.81
[33]	3.97991	0.42983	1.79	0.68

Now, we make numerical comparison with some existing methods [18, 27–33]. The results displayed in Table 3 are for the simulations with the parameters $c = 0.1$, $x \in [-40, 60]$, $\tau = 0.1$, $h = 0.1$, $T = 20$ and homogeneous boundary conditions. In this case, the exact invariants $I_1 = \int u\mathrm{d}x \approx 3.9799497484$ and $I_3 = \int(\gamma u^3/6 + au^2/2)\mathrm{d}x \approx 0.4298345728$. Obviously, the LEP schemes (25) and (26) have the same solution accuracy and exhibit much more accurate solutions than the other schemes.

Example 4. In the previous examples, we consider the problems with the periodic/homogeneous boundary conditions. To illustrate the validity of the present local structure-preserving algorithms, the Sine-Gordon equation, $u_{tt} - u_{xx} = -\sin u$ without periodic/homogeneous boundary condition will be solved. The Sine-Gordon equation is also a multi-symplectic Hamiltonian system with the two skew-symmetric matrices

$$M = \begin{pmatrix} 0 & -1 & 0 & 0 \\ 1 & 0 & 0 & 0 \\ 0 & 0 & 0 & 1 \\ 0 & 0 & -1 & 0 \end{pmatrix}, \quad K = \begin{pmatrix} 0 & 0 & -1 & 0 \\ 0 & 0 & 0 & 1 \\ 1 & 0 & 0 & 0 \\ 0 & -1 & 0 & 0 \end{pmatrix},$$

and $S(z) = v^2/2 - w^2/2 - \cos u$, $z = (u, v, w, \phi)^T$. Taking the splitting matrix $\widehat{K}$ as an upper triangular matrix of K leads to

$$\begin{cases} -\delta_t^+ v_j^n - A_t \delta_x^+ w_j^n = f_1(\cos u_j^{n+1}, \cos u_j^n), \\ \delta_t^+ u_j^n + A_t \delta_x^+ \phi_j^n = A_t v_j^n, \\ \delta_t^+ \phi_j^n + A_t \delta_x^- u_j^n = -A_t w_j^n, \\ \delta_t^+ w_j^n - A_t \delta_x^- v_j^n = 0, \end{cases} \tag{29}$$

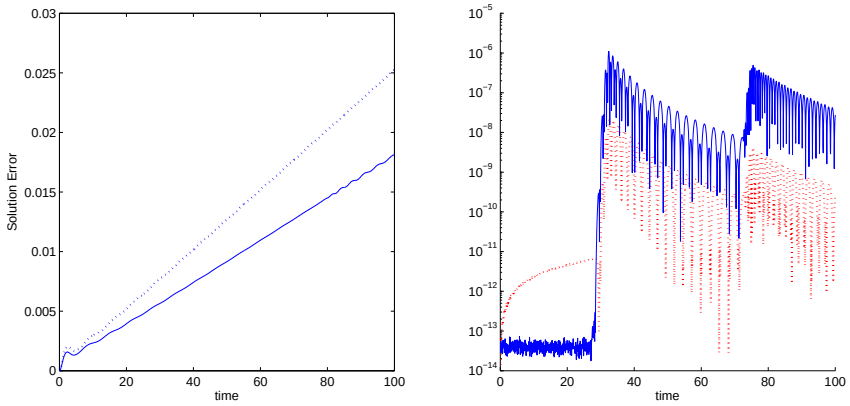

Figure 4: The numerical results for Sine-Gordon equation obtained by the LEP scheme (30). Left: maximal (solid line) and averaged (dotted line) errors in solution. Right: local energy (blue solid line) and the global energy error (red dotted line).

with

$$f_1(s,r) = \begin{cases} -(\cos s - \cos r)/(r-s), & s \neq r, \\ 1, & s = r, \end{cases}$$

which can be written into a compact form

$$\delta_t^{+2} u_j^n - \delta_x^+ \delta_x^- A_t^2 u_j^n = A_t f_1(\cos u_j^{n+1}, \cos u_j^n). \tag{30}$$

The Sine-Gordon equation has an analytical solution in the form of $u(x,t) = 4\arctan(\exp(\frac{x-ct}{\sqrt{1-c^2}}))$. In the following simulation, we consider the initial condition $u_0(x) = u(x,0)$ with $c = 0.2$ and $x \in [-30, 70]$. The simulation is carried out with equispaced $h = 0.1$ and $\tau = 0.05$ till $T = 100$. Fig. 4 shows the obtained results on the errors in solution, local energy and the errors in global energy. Both the maximal and average errors in solution increase linearly, but they are still satisfactory until $T = 100$ (less than 0.025). The local energy and the error in global energy versus time shown in Fig. 4 (right) confirm that the proposed scheme are also effective for the problem with general boundary condition.

3 Local structure-preserving methods for multi-dimensional problem and applications

Many PDEs such as two-/three-dimensional (2D/3D) Gross-Pitaevskii equation and Maxwell's equations can be recast into the form of (1). The present LEP and LMP integrators for the 1D multi-symplectic Hamiltonian PDE (7) can be extended to d-dimensional case (1) directly.

Let $z_{j_1,\cdots,j_d}^n$ be a numerical approximation to $z(x_{1_{j_1}}, \cdots, x_{d_{j_d}}, t_n)$ where $x_{l\,j_l+1} = x_{l_{j_l}} + h_l$, $l = 1, 2, \cdots, d$, and $t_{n+1} = t_n + \tau$. For the simplicity, in the most of the equations we present, one of the indices is held constant, in which case, we drop it from the notation. Denote the forward and backward Euler finite difference operators in x_l direction by $\delta_{x_l}^+$ and $\delta_{x_l}^-$ respectively. As the splitting matrices $\widehat{M}_l$ and $\widehat{K}_l$ satisfy (3), we obtain a LEP integrator

$$M\delta_t^+ z + \sum_{l=1}^{d} \widehat{K}_l A_t \delta_{x_l}^+ z - \sum_{l=1}^{d} \widehat{K}_l^T A_t \delta_{x_l}^- z = \int_0^1 \nabla_z S\left(z + \xi\tau\delta_t^+ z\right) \mathrm{d}\xi, \tag{31}$$

which has a local energy conservation law

$$\delta_t^+ E + \sum_{l=1}^{d} \delta_{x_l}^+ F_l^{n+\frac{1}{2}} = 0, \tag{32}$$

where $E = S(z) + \sum_{l=1}^{d} (\delta_{x_l}^- z)^T \widehat{K}_l z$ and $F_l^{n+\frac{1}{2}} = -(\delta_t^+ z_{j_l-1})^T \widehat{K}_1 A_t z$, and a x_l-direction LMP integrator

$$\widehat{M}\delta_t^+ A_{x_l} z - \widehat{M}^T \delta_t^- A_{x_l} z + K_l \delta_{x_l}^+ z + \sum_{j=1, j\neq l}^{d} (\widehat{K}_j \delta_{x_j}^+ A_{x_l} z - \widehat{K}_j^T \delta_{x_j}^- A_{x_l} z) \tag{33}$$

$$= \int_0^1 \nabla_z S(z + \xi h_l \delta_{x_l}^+ z) \mathrm{d}\xi, \ l = 1, 2, \cdots, d,$$

which admits the x_l-direction discrete local momentum conservation law

$$\delta_t^+ I_{l_{j_l+\frac{1}{2}}} + \delta_{x_l}^+ G_l + \sum_{k=1, k\neq l}^{d} \delta_{x_k}^+ \tilde{G}_{l,k} = 0, \tag{34}$$

where $I_{l_{j_l+\frac{1}{2}}} = -(\delta_{x_l}^+ z^{n-1})^T \widehat{M} A_{x_l} z$, $G_l = S(z) + (\delta_t^- z)^T \widehat{M} z + \sum_{k=1, k\neq l}^{d} (\delta_{x_k}^- z)^T \widehat{K}_k z$ and $\tilde{G}_{l,k} = -(\delta_{x_l}^+ z_{j_k-1})^T \widehat{K}_k z$.

Example 5. Consider the 2D NLS equation

$$i\psi_t + \alpha\Delta\psi + V'(|\psi|^2, \mathbf{x})\psi = 0, \tag{35}$$

where the symbol $'$ represents the derivative of V with respect to the first variable and the Laplace operator $\Delta = \partial_{x_1}^2 + \partial_{x_2}^2$. Let $\psi = p + iq$, real-valued p and q are real and imaginary parts of ψ, respectively. Introducing $v^{x_1} = \partial_{x_1} p$, $w^{x_1} = \partial_{x_1} q$, $v^{x_2} = \partial_{x_2} p$ and $w^{x_2} = \partial_{x_2} q$, we transform (35) into 2D multi-symplectic Hamiltonian form where $S(z) = \frac{1}{2} V(p^2 + q^2, \mathbf{x}) + \frac{\alpha}{2}((v^{x_1})^2 + (w^{x_1})^2 + (v^{x_2})^2 + (w^{x_2})^2)$, $z = (p, q, v^{x_1}, w^{x_1}, v^{x_2}, w^{x_2})$, and the skew-symmetric matrices ($\in \mathbb{R}^{6\times 6}$) are

$$M = \begin{pmatrix} J & 0 & 0 \\ 0 & 0 & 0 \\ 0 & 0 & 0 \end{pmatrix}, \ K_1 = \begin{pmatrix} 0 & -\alpha I & 0 \\ \alpha I & 0 & 0 \\ 0 & 0 & 0 \end{pmatrix}, \ K_2 = \begin{pmatrix} 0 & 0 & -\alpha I \\ 0 & 0 & 0 \\ \alpha I & 0 & 0 \end{pmatrix},$$

with matrices J, $I \in \mathbb{R}^{2\times 2}$ (see Example 2). Let the splitting matrices $\widehat{K}_l$, $l = 1, 2$, be upper triangular matrices of K_l, respectively. Applying the integrator (31) to this problem, and then eliminating the auxiliary variables give a LEP scheme

$$\begin{cases} \delta_t q - \alpha \underline{\Delta} A_t p = \int_0^1 V' \left((p + \xi\delta_t^+ p)^2 + (q + \xi\delta_t^+ q)^2\right)(p + \xi\delta_t^+ p)\mathrm{d}\xi, \\ -\delta_t p - \alpha \underline{\Delta} A_t q = \int_0^1 V' \left((p + \xi\delta_t^+ p)^2 + (q + \xi\delta_t^+ q)^2\right)(q + \xi\delta_t^+ q)\mathrm{d}\xi, \end{cases} \tag{36}$$

where the operator $\underline{\Delta} = \delta_{x_1}^+ \delta_{x_1}^- + \delta_{x_2}^+ \delta_{x_2}^-$ represents a discrete version of the continuous Laplace operator. Similarly, choosing the splitting matrices $\widehat{K}_l = K_l/2$, $l = 1, 2$, will read another LEP scheme (only need to replace the discrete Laplace operator in (36) by $\underline{\Delta} = \bar{\delta}_{x_1}^+ \bar{\delta}_{x_1}^- + \bar{\delta}_{x_2}^+ \bar{\delta}_{x_2}^-$) for the 2D NLS equation. The two schemes are referred to as LEP-1 and LEP-2, respectively.

Consider $\alpha = 1/2$ and $V(|\psi|^2, \mathbf{x}) = V_1(\mathbf{x})|\psi|^2 + \beta|\psi|^4/2$. The equation (35) becomes the Gross-Pitaevskii (G-P) equation which is an important mean field model for the dynamics of a dilute gas Bose-Einstein condensate. The parameter β determines whether the G-P equation is attractive ($\beta > 0$) or repulsive ($\beta < 0$). For the G-P equation, the nonlinear term are integrated exactly so that the LEP-1 and -2 schemes become

$$i\delta_t^+ \psi^n + \alpha \underline{\Delta} A_t \psi^n + V_1(x_{1j_1}, x_{2j_2}) A_t \psi + \beta g(\psi^{n+1}, \psi^n, p^{n+1}, p^n) = 0. \tag{37}$$

We first consider the attractive case with $\beta = 1$, $V_1(\mathbf{x}) = -(x_1^2 + x_2^2)/2 - 2\exp(-(x_1^2 + x_2^2))$ and the initial condition given by $\psi(\mathbf{x}, 0) = \sqrt{2}\exp(-(x_1^2 + x_2^2)/2)$. For this initial problem, the G-P equation has an solution $\psi(\mathbf{x}, t) = \sqrt{2}\exp(-(x_1^2 + x_2^2)/2 - it)$. We set the spatial domain $[-6, 6]^2$ which is divided into 60×60 grids and the temporal interval $[0, 5]$ with $\tau = 0.005$. Fig. 5 (left) shows that the maximal errors in solution increase as time evolves and the maximal error of LEP-2 grows faster than that of LEP-1. The residuals in global energy shown in Fig. 5 (right) confirm the LEP-1 and -2 schemes are energy-preserving numerically.

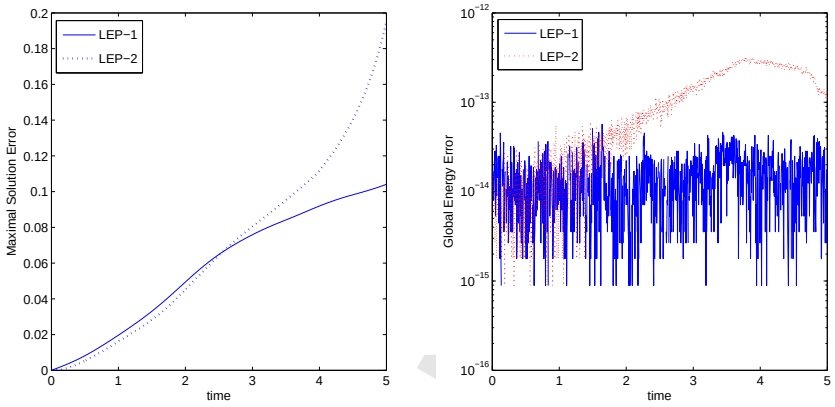

Figure 5: Numerical results for the G-P equation (attractive case, $\beta = 1$). Left: the maximal errors in solution. Right: the global energy error.

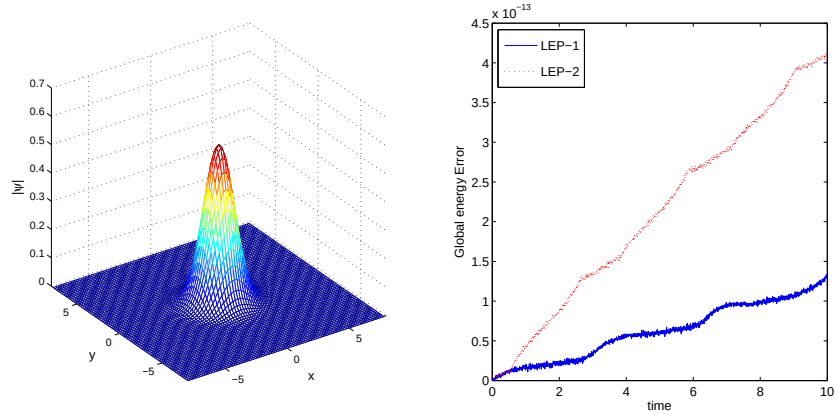

Figure 6: Numerical results for the G-P equation (repulsive case, $\beta = -2$). Left: the profile of $|\psi|$ at $T = 10$. Right: the global energy error.

Table 4: The numerical results obtained by the LEP schemes and the existing symplectic schemes: $h_1 = h_2 = \pi/32$, $T = 100$.

Method	τ	L_∞-error	L_2-error	$\lvert\mathcal{E}^n - \mathcal{E}^0\rvert$
LEP-1	0.05	9.52e-5	1.18e-3	3.95e-12
	0.025	2.35e-5	3.22e-4	5.24e-12
	0.0125	9.79e-6	1.12e-4	6.07e-12
LEP-2	0.05	6.01e-5	6.85e-4	8.40e-11
	0.025	1.62e-5	1.73e-4	7.32e-10
	0.0125	5.14e-6	3.53e-5	6.86e-11
SY-1	0.05	2.48e-4	5.29e-3	9.40e-4
	0.025	7.44e-5	2.77e-3	2.56e-4
	0.0125	2.64e-5	1.64e-3	8.69e-5
SY-2	0.05	3.29e-3	4.73e-2	4.81e-2
	0.025	1.47e-3	1.85e-2	1.14e-2
	0.0125	1.34e-4	4.33e-3	6.18e-3
SY-3	0.05	9.82e-5	2.97e-3	1.33e-4
	0.025	8.19e-5	4.36e-3	6.30e-4
	0.0125	3.29e-5	2.26e-3	1.71e-4

We second consider the repulsive case with $\beta = -2$, $V_1 = -(x_1^2 + x_2^2)/2$ and the initial condition $\psi(\mathbf{x}, 0) = \exp(-(x_1^2 + x_2^2)/2)/\sqrt{\pi}$. The computational domain is taken as $[-8, 8]^2 \times [0, 10]$ and the mesh grid sizes $\tau = 0.005$ and $h_1 = h_2 = 0.2$. Fig. 6 (left) shows the profile of numerical solution $|\psi|$ at $T = 10$ and Fig. 6 (right) displays the residuals of discrete energy versus time. The results imply that the global energy of each scheme remains a constant throughout computations.

Lastly, we consider the G-P equation with $\beta = -1$ and $V_1 = \sin^2 x_1 \sin^2 x_2 - 1$ imposed on initial condition $\psi(\mathbf{x}, 0) = \sin x_1 \sin x_2$, $\mathbf{x} \in [0, 2\pi]^2$. In this case, the analytic solution is $\psi(\mathbf{x}, t) = \exp(2it) \sin x_1 \sin x_2$. Kong et. al [34] have developed three symplectic schemes for this problem, which will be referred as SY-1, SY-2 and SY-3 in this paper. Next, we make some numerical comparisons (see Table 4) between the proposed LEP schemes and the symplectic schemes. One can see that the solution of our schemes are more accurate than those of symplectic schemes. In addition, the LEP schemes successfully integrate the problem with the energy strictly kept.

Example 6. Now, we consider the NLS equation (35) in 3D case ($\mathbf{x} = (x_1, x_2, x_3)$, $\Delta = \partial_{x_1}^2 + \partial_{x_2}^2 + \partial_{x_3}^2$). The multi-symplectic form of this problem is easy to be obtained. An application of the present LEP integrator (31) to the obtained multi-symplectic form yields a similar scheme in Example 5 where the discrete Laplace operator should be $\underline{\Delta} = \delta_{x_1}^+ \delta_{x_1}^- + \delta_{x_2}^+ \delta_{x_2}^- + \delta_{x_3}^+ \delta_{x_3}^-$. To show the numerical performance of the obtained LEP scheme, we solve the 3D NLS equation with $V_1(\mathbf{x}) = \sin^2 x_1 \sin^2 x_2 \sin^2 x_3 - 1$, $\beta = -1$ and the initial condition $u(\mathbf{x}, 0) = \sin x_1 \sin x_2 \sin x_3$, $\mathbf{x} \in [0, 2\pi]^3$. In this case, the analytical solution is $u(\mathbf{x}, t) = \sin x_1 \sin x_2 \sin x_3 \exp(-5it/2)$. The simulation is carried out with mesh sizes $\tau = 0.005$ and $h_1 = h_2 = h_3 = \pi/32$ up to $T = 10$. The numerical results are illustrated with Fig. 7, from which one can see that the LEP scheme exhibits good numerical performance.

Example 7. Three-dimensional Maxwell's equations in units for the electromagnetic field in a vacuum are

$$\frac{\partial \mathbf{E}}{\partial t} = \frac{1}{\varepsilon} \nabla \times \mathbf{H}, \quad \frac{\partial \mathbf{H}}{\partial t} = -\frac{1}{\mu} \nabla \times \mathbf{E}, \tag{38}$$

which can be recast as a multi-symplectic form where $S(z) = 0$, $z = (\mathbf{H}^T, \mathbf{E}^T)^T$, I_3 designates the 3×3 unit matrix and

$$M = \begin{pmatrix} 0 & -I_3 \\ I_3 & 0 \end{pmatrix}, \quad K_l = \begin{pmatrix} \varepsilon^{-1} R_l & 0 \\ 0 & \mu^{-1} R_l \end{pmatrix}, \quad l = 1, 2, 3,$$

$$R_1 = \begin{pmatrix} 0 & 0 & 0 \\ 0 & 0 & -1 \\ 0 & 1 & 0 \end{pmatrix}, \quad R_2 = \begin{pmatrix} 0 & 0 & 1 \\ 0 & 0 & 0 \\ -1 & 0 & 0 \end{pmatrix}, \quad R_3 = \begin{pmatrix} 0 & -1 & 0 \\ 1 & 0 & 0 \\ 0 & 0 & 0 \end{pmatrix}.$$

Taking the splitting matrices K_l, $l = 1, 2, 3$ as upper triangular matrices of K_l, and then applying the integrator (31) to the problem give a LEP scheme for Maxwell's equations, which preserves a discrete energy conservation law $\mathcal{E}^n = \varepsilon \|\mathbf{E}^n\|^2 + \mu \|\mathbf{H}^n\|^2 = \cdots = \mathcal{E}^0 = \varepsilon \|\mathbf{E}^0\|^2 + \mu \|\mathbf{H}^0\|^2$. Preservation of energy is numerically confirmed by an experiment with random initial data on a regular grid with 32 points in

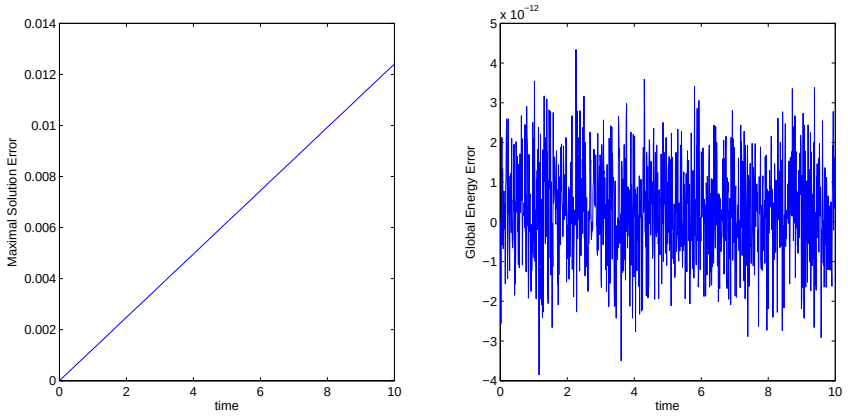

Figure 7: The error in solution (left) and global energy error versus time (right) for the 3D NLS equation.

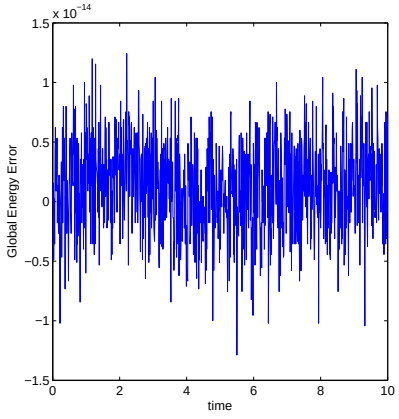

Figure 8: Three-dimensional Maxwell's equations: energy error vs time, the LEP method.

every direction, periodic boundary condition on the unit cube and constants $\varepsilon = \mu = 1$. The results of the LEP scheme with $\tau = 0.01$ can be seen in Fig. 8.

4 Numerical dispersion

As one would expect, the nonlinearity of (1) makes the study of numerical solutions for the problem more difficult. Hence, the aim of this section is to conduct an analysis of the LEP discretization method for the linear equation

$$M\partial_t z + K\partial_x z = Az, \tag{39}$$

where A is symmetric. Applying the LEP scheme to (39) yields

$$M\delta_t^+ z_j^n + \widehat{K} A_t \delta_x^+ z_j^n - \widehat{K}^T A_t \delta_x^- z_j^n = A A_t z_j^n. \tag{40}$$

In the following, we only consider the choice of $\widehat{K} = K/2$.

Theorem 4.1. *Numerical solutions of the scheme (40) satisfy the numerical dispersion relation*

$$\det(i\omega M + i\chi K - A) = 0,$$

where $\omega = 2\sin(\Omega\tau/2)/\tau$ *and* $\chi = \sin(Xh)/h$ *for* $-\pi < \Omega\tau < \pi$ *and* $-\pi < Xh < \pi$.

Proof. We substitute a standard solution ansatz of the form $z(x,t) = e^{i(\Omega n\tau + Xjh)}\mathrm{v}$ into (40) where v is a d_1-dimensional complex-valued vector. This yields

$$\left(M\frac{e^{i\Omega\tau/2} - e^{-i\Omega\tau/2}}{\tau} + K\frac{e^{iXh} - e^{-iXh}}{2h} - A\right)\mathrm{v} = 0. \tag{41}$$

The proof is completed. □

We now investigate the behavior of the LEP discretization for the linear wave equation

$$u_{tt} = u_{xx}. \tag{42}$$

The numerical dispersion relation is given by

$$\tan^2\left(\frac{\Omega\tau}{2}\right) = \frac{\tau^2}{h^2}\sin^2\left(\frac{Xh}{2}\right)$$

and is real-valued for any value of τ/h. The numerical dispersion relation has no spurious root for given Ω and X, and converges to the exact dispersion relation as $\tau,\ h \to 0$. Frank et. al [35] proposed an explicit midpoint (EMP) scheme by applying the explicit midpoint rule in both time and space, from which one has the numerical relation

$$\sin^2(\Omega\tau) = \frac{\tau^2}{h^2}\sin^2(Xh).$$

It is clear that there are spurious roots for given Ω and X, respectively. To eliminate the spurious roots for X or Ω in the numerical dispersion relation of the EMP discretization, the authors [35] applied the symplectic Störmer-Verlet (SV) method in space and yielded the numerical dispersion relation

$$\sin^2(\Omega\tau) = \frac{4\tau^2}{h^2}\sin^2(\frac{Xh}{2}),$$

while application in time implies

$$\sin^2(\frac{\Omega\tau}{2}) = \frac{\tau^2}{4h^2}\sin^2(Xh).$$

As shown in Fig. 9, the numerical dispersion relation of the LEP discretization has as many solution branches as the exact dispersion relation, while all the other discretizations have spurious roots in their numerical dispersion relations. The spurious branches (roots) are due to the multistep EMP method. Those spurious resonances can lead to instabilities of the method under small perturbations in the same manner as analytic resonances can give rise to instabilities.

5 Conclusion

Many PDEs such as the KdV equation, G-P equation, Maxwell's equations and so on can be reformed into the general multi-symplectic Hamiltonian system which has three local conservation laws, including MSCL, LECL and LMCL. These conservation laws are independent of boundary conditions, so that they are more essential than the global ones. Naturally, it is desired to develop a numerical integrator holding one or more discrete versions of the local conservation laws for the general multi-symplectic Hamiltonian system. The first proposed local structure-preserving algorithm is multi-symplectic scheme, but it cannot conserve the local energy and momentum well. In order to capture the local energy/momentum of the system exactly, we have developed some LEP/LMP algorithms in [17, 18]. However, their less positive features are fully implicit, strongly restrict in mesh grids and inconvenient to establish the error estimate. In this paper, based on the symplectic and DG discretizations, we develop some new LEP/LMP integrators that are applicable to the entire class of multi-symplectic Hamiltonian PDE. There are some merits of the proposed integrators. For example, they are valid for both odd and even grid points; they are constructed on the grid points which allows us to establish the error estimate conveniently; The LMP integrator is fully explicit or linearly implicit as applying it to some particular Hamiltonian PDEs. In order to test the effectiveness of the proposed LEP and LMP integrators, we apply them to many PDEs,

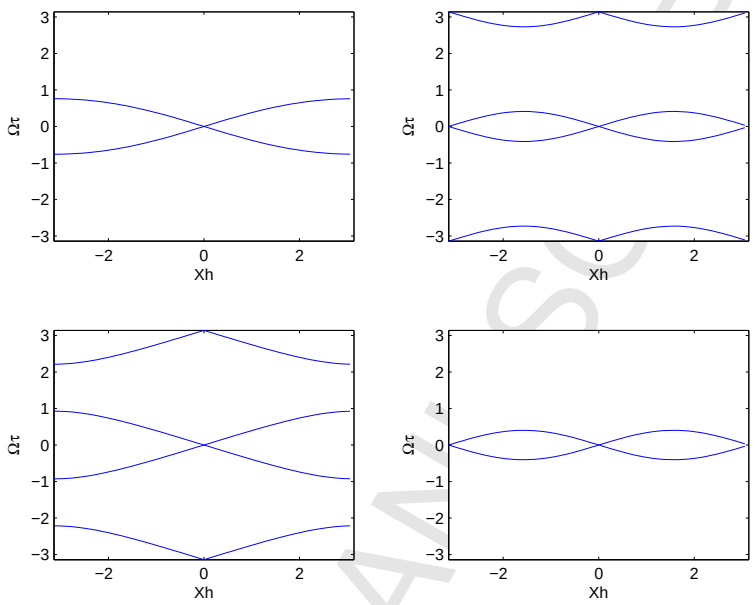

Figure 9: The numerical dispersion relations for different discretizations with $\tau/h = 2/5$. Top-left: the LEP discretization; Top-right: EMP discretization in both time and space; Bottom-left: SV discretization in space combined with EMP discretization in time; Bottom-right: an EMP discretization in space and a SV discretization in time.

such as the KdV equation, RLW equation, Schrödinger equation, G-P equation, Maxwell's equations and so on, and carry out many numerical experiments. Numerical results confirm the theoretical analysis. In the present paper, we mainly focus on construction of the LEP and LMP integrators by the AVF method. And thus the given LEP integrator is always implicit. To develop fully explicit or linearly implicit LEP integrator, we could replace the AVF method by other DG methods such as the coordinate increment DG method.

Acknowledgements

The work is supported by Natural Science Foundation of Jiangsu Province of China, NNSF of China (11771213) and Jiangsu Overseas Visiting Scholar Program for University Prominent Young & Middle-aged Teachers and Presidents. The authors would like to express sincere gratitude to the referee for the insightful comments and suggestions which help to improve the paper.

References

[1] T.J. Bridges, S. Reich, Multi-symplectic integrators: numerical schemes for Hamiltonian PDEs that conserve symplecticity, Phys. Lett. A 284 (2001) 184-193.

[2] B. Leimkuhler, S. Reich, Simulating Hamiltonian dynamics, Cambridge Monogr. Appl. Comput. Math. Cambridge University Press, Cambridge, UK, 2004.

[3] U.M. Ascher, R.I. McLachlan, Multisymplectic box schemes and the Korteweg-de Veries equation, Appl. Numer. Math. 48 (2004) 255-269.

[4] D. Cohen, B. Owren, X. Raynaud, Multi-symplectic integration of the Camassa-Holm equation, J. Comput. Phys. 227 (2008) 5492-5512.

[5] J.X. Cai, A new explicit multisymplectic scheme for the regularized long-wave equation, J. Math. Phys. 50 (2009) 013535:1-16.

[6] J.B. Chen, M.Z. Qin, Y.F. Tang, Symplectic and multi-symplectic methods for the nonlinear Schrödinger equation, Comput. Math. Appl. 43 (2002) 1095-1106.

[7] J.X. Cai, C.Z. Bai, H.H. Zhang, Decoupled local/global energy-preserving schemes for the N-coupled nonlinear Schrödinger equations, J. Comput. Phys. 374 (2018) 281-299.

[8] J.X. Cai, Y.S. Wang, Y.Z. Gong, Numerical Analysis of AVF methods for three-dimensional time-domain Maxwell's equations, J. Sci. Comput. 66 (2016) 141-176.

[9] L.H. Kong, J.L. Hong, J.J. Zhang, Splitting multisymplectic integrators for Maxwell's equations, J. Comput. Phys. 229 (2010) 4259-4278.

[10] B.E. Moore, S. Reich, Backward error analysis for multi-symplectic integration methods, Numer. Math. 95 (2003) 625-652.

[11] J.B. Chen, M. Z. Qin, Multi-symplectic Fourier pseudo spectral method for the nonlinear Schrödinger equation, Electron. Trans. Numer. Anal. 12 (2001) 193-204.

[12] R.I. McLachlan, M.C. Wilkins, The multi-symplectic diamond scheme, SIAM J. Sci. Comput. 37 (2015) A369-A390.

[13] D. Furihata, Discrete variational derivative method: A structure-preserving numerical method for partial differential equations, Chapman & Hall/CRC, Boca Raton, (2011).

[14] Y. Miyatake, T. Matsuo, A general framework for finding energy dissipative/conservative H^1-Galerkin schemes and their underlying H^1-weak forms for nonlinear evolution equations, BIT Numer. Math. 54 (2014) 1119-1154.

[15] E. Celledoni, V. Grimm, R.I. McLaren, D. O'Neale, B. Owren, G.R.W. Quispel, Perserving energy resp. dissipation in numerical PDEs using the "Average Vector Field" method, J. Comput. Phys. 231 (2012) 6770-6789.

[16] Y.S. Wang, B. Wang, M.Z. Qin, Local structure-preserving algorithms for partial differential equations, Sci. Chin. Ser. A Math. 51 (2008) 2115-2136.

[17] J.X. Cai, Y.S. Wang, H. Liang, Local energy-preserving and momentum-preserving algorithms for coupled nonlinear Schrödinger equations, J. Comput. Phys. 239 (2013) 30-50.

[18] Y.Z. Gong, J.X. Cai, Y.S. Wang, Some new structure-preserving algorithms for general multi-symplectic formulations of Hamiltonian PDEs, J. Comput. Phys. 279 (2014) 80-102.

[19] B. Byland, Multisymplectic integration, Ph.D. Thesis, Massey University, New Zealand, 2007.

[20] T. Itoh, K. Abe, Hamiltonian-conserving discrete canonical equations based on variational difference quotients, J. Comput. Phys., 76 (1998) 85-102.

[21] O. Gonzalez, J.C. Simo, On the stability of symplectic and energy-momentum algorithms for non-linear Hamiltonian systems with symmetry, Comput. Methods Appl. Mech. Eng. 134 (1996) 197-222.

[22] G.R.W. Quispel, D.I. McLaren, A new class of energy-preserving numerical integration method, J. Phys. A 41 (2008) 045206:1-7.

[23] R.I. McLachlan, G.R.W. Quispel, N. Robidoux, Geometric integration using discrete gradients, Philos. Trans. R. Soc. A 357 (1999) 1021-1046.

[24] R.I. McLachlan, G.R.W. Quispel, G.S. Turner, Numerical integrators that preserve symmetries and reversing symmetries, SIAM J. Numer. Anal. 35 (1998) 586-599.

[25] P.F. Zhao, M.Z. Qin, Multisymplectic geometry and multisymplectic Preissmann scheme for the KdV equation, J. Phys. A: Math. Gen. 33 (2000) 3613-3626.

[26] U.M. Ascher, R.I. McLachlan, On symplectic and multisymplectic schemes for the KdV equation, J. Sci. Comput. 25 (2005) 83-104.

[27] J.X. Cai, Q. Hong, Efficient local structure-preserving schemes for the RLW-type equation, Numer. Meth. Part. D. E. 33 (2017) 1678-1691.

[28] A. Esen, S. Kutluay, Application of a lumped Galerkin method to the regularized long wave equation, Appl. Math. Comput. 174 (2006) 833-845.

[29] L.R.T. Gardner, G.A. Gardner, A. Dogan, A least-squares finite element scheme for the RLW equation, Commun. Numer. Meth. Eng. 12 (1996) 795-804.

[30] A. Dogan, Numerical solution of RLW equation using linear finite elements within Galerkin's method, Appl. Math. Model. 26 (2002) 771-783.

[31] K.R. Raslan, A computational method for the regularized long wave (RLW) equation, Appl. Math. Comput. 167 (2005) 1101-1118.

[32] S.I. Zaki, Solitary waves of the splitted RLW equation, Comput. Phys. Commun. 138 (2001) 80-91.

[33] R. Mokhtari, M. Mohammadi, Numerical solution of GRLW equation using Sinc-collocation method, Comput. Phys. Commun. 181 (2010) 1266-1274.

[34] L.H. Kong, J.L. Hong, F.F. Fu, J. Chen, Symplectic structure-preserving integrators for the two-dimensional Gross-Pitaevskii equation for BEC, J. Comput. Appl. Math. 235 (2011) 4937-4948.

[35] J. Frank, B.E. Moore, S. Reich, Linear PDEs and numerical methods that preserve a multisymplectic conservation law, SIAM J. Sci. Comput. 28 (2006) 260-277.